Nanoscope based on nanowaveguides

A. H. Rose, B. M. Wirth, R. E. Hatem, A. P. Rashed Ahmed, M. J. Burns, M. J. Naughton, and K. Kempa*

Department of Physics, Boston College, 140 Commonwealth Avenue, Chestnut Hill, Massachusetts 02467, USA
*kempa@bc.edu

Abstract: The far field spatial resolution of conventional optical lenses is of the order of the wavelength of light, due to loss in the far field of evanescent, near electromagnetic field components. We show that subwavelength details can be restored in the far field with an array of divergent nanowaveguides, which map the discretized, subwavelength image of an object into a magnified image observable with a conventional optical microscope. We demonstrate in simulations that metallic nanowires, nanocoaxes, and nanogrooves can be used as such nanowaveguides. Thus, an optical microscope capable of subwavelength resolution — a nanoscope — can be produced, with possible applications in a variety of fields where nanoscale optical imaging is of value.

©2014 Optical Society of America

OCIS codes: (160.1190) Anisotropic optical materials; (180.4243) Near-field microscopy; (230.7370) Waveguides; (240.6680) Surface plasmons; (250.5403) Plasmonics; (310.6628) Subwavelength structures, nanostructures.

References and links

1. E. Abbe, "Über einen neuen beleuchtungsapparat am mikroskop," Archiv Für Mmikroskopische Anatomie. **9**(1), 469–480 (1873).
2. Max Born and Emil Wolf, *Principles of Optics,* (Cambridge University, 1997).
3. J. B. Pendry, "Negative refraction makes a perfect lens," Phys. Rev. Lett. **85**(18), 3966–3969 (2000).
4. Z. Jacob, L. V. Alekseyev, and E. Narimanov, "*Optical Hyperlens*: Far-field imaging beyond the diffraction limit," Opt. Express **14**(18), 8247–8256 (2006).
5. A. Salandrino and N. Engheta, "Far-field subdiffraction optical microscopy using metamaterial crystals: theory and simulations," Phys. Rev. B **74**(7), 075103 (2006).
6. Z. Liu, H. Lee, Y. Xiong, C. Sun, and X. Zhang, "Far-field optical hyperlens magnifying sub-diffraction-limited objects," Science **315**(5819), 1686 (2007).
7. I. I. Smolyaninov, Y. J. Hung, and C. C. Davis, "Magnifying superlens in the visible frequency range," Science **315**(5819), 1699–1701 (2007).
8. M. G. Silveirinha, P. A. Belov, and C. R. Simovski, "Subwavelength imaging at infrared frequencies using an array of metallic nanorods," Phys. Rev. B **75**(3), 035108 (2007).
9. G. Shvets, S. Trendafilov, J. B. Pendry, and A. Sarychev, "Guiding, focusing, and sensing on the subwavelength scale using metallic wire arrays," Phys. Rev. Lett. **99**(5), 053903 (2007).
10. Y. Zhao, "Investigation of image magnification properties of hyperlenses formed by a tapered array of metallic wires using a spatially dispersive finite-difference time-domain method in cylindrical coordinates," J. Opt. A. Pure Appl. Opt. **14**, 035102 (2012).
11. S. Kawata, A. Ono, and P. Verma, "Subwavelength colour imaging with a metallic nanolens," Nat. Photonics **2**(7), 438–442 (2008).
12. K. Kempa, X. Wang, Z. F. Ren, and M. J. Naughton, "Discretely guided electromagnetic effective medium," Appl. Phys. Lett. **92**(4), 043114 (2008).
13. J. Rybczynski, K. Kempa, A. Herczynski, Y. Wang, M. J. Naughton, Z. F. Ren, Z. P. Huang, D. Cai, and M. Giersig, "Subwavelength waveguide for visible light," Appl. Phys. Lett. **90**(2), 021104 (2007).
14. B. Rizal, F. Ye, P. Dhakal, T. C. Chiles, S. Shepard, G. McMahon, M. J. Burns, and M. J. Naughton, "Imprint-templated nanocoax array architecture: fabrication and utilization," in *Nano-Optics for Enhancing Light-Matter Interactions on a Molecular Scale*, B. Di Bartolo, J. Collins, and L. Silvestri, eds. (Springer, Dordrecht, 2013), Chap. 18.
15. H. Ditlbacher, A. Hohenau, D. Wagner, U. Kreibig, M. Rogers, F. Hofer, F. R. Aussenegg, and J. R. Krenn, "Silver nanowires as surface plasmon resonators," Phys. Rev. Lett. **95**(25), 257403 (2005).
16. A. Manjavacas and F. J. García de Abajo, "Robust plasmon waveguides in strongly interacting nanowire arrays," Nano Lett. **9**(4), 1285–1289 (2009).

17. Y. Peng and K. Kempa, "Controlling light propagation with nanowires," Appl. Phys. Lett. **100**(17), 171903 (2012).
18. M. Kuttge, F. J. García de Abajo, and A. Polman, "How grooves reflect and confine surfaceplasmon polaritons," Opt. Express **17**(12), 10385–10392 (2009).
19. C. L. C. Smith, B. Desiatov, I. Goykmann, I. Fernandez-Cuesta, U. Levy, and A. Kristensen, "Plasmonic V-groove waveguides with Bragg grating filters via nanoimprint lithography," Opt. Express **20**(5), 5696–5706 (2012).
20. J. Jin, *The Finite Element Method in Electromagnetics*, (Wiley-IEEE, 2002).
21. "We employ CST Microwave Studio, with material parameters for metals from P. B. Johnson and R. W. Christy, "Optical constants of the noble metals," Phys. Rev. B **6**, 4370–4379 (1972).
22. The transmitted field intensity is defined as the normalized magnitude of the time-averaged Poynting vector (extracted from simulation), averaged over the distal end of the wire.

With conventional lenses, image details much smaller than the wavelength of the light being employed in microscopy propagate only as evanescent waves and thus are lost at distances beyond a wavelength, or the far field [1,2]. However, there is no fundamental limitation on the recovery of this lost information, and a far field superlens has been proposed based on a negative refractive index medium [3]. The lack of negative refractive media operational in the optical frequency range has thus far prevented experimental demonstration of such a far field superlens. Another way to achieve a far field superlens is to place a near field optical magnifier (NFOM) within the near field of an image, configured so that the output of the magnifier is no longer subwavelength and can thus be propagated into the far field. Metamaterial NFOMs based on alternating thin metallic and dielectric films have been proposed [4,5] and experimentally demonstrated [6,7]. NFOMs based on arrays [8], including divergent [9,10], of continuous nanowires with inter-wire wave propagation and segmented wires capable of multi-wavelength operation in the optical regime [11] have also been proposed and simulated but not yet experimentally demonstrated. Another NFOM, based on divergent arrays of coaxial nanowaveguides, with exclusive intra-waveguide wave propagation (either by TEM photon modes or surface plasmon polaritons) has been proposed by some of us [12]. An NFOM based on generalized nanowaveguides is shown schematically in Fig. 1 as a part of a nanoscale microscope, or nanoscope.

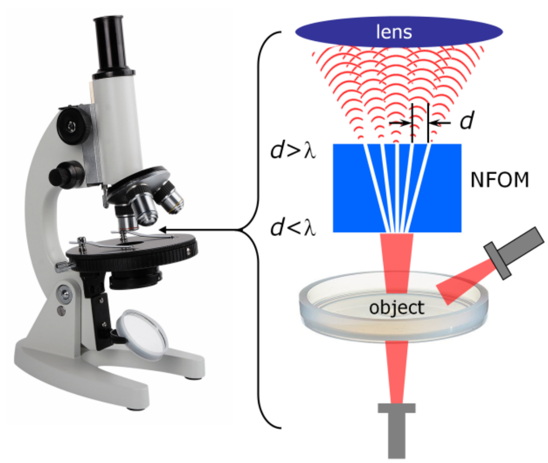

Fig. 1. Schematic of imaging with proposed near field optical magnifier comprised of nanowaveguides (white lines) supported by dielectric filler (blue). The subwavelength-size "object" is placed at the input ends of the nanowaveguides array (having waveguide separation $d < \lambda$). When illuminated, the image of the object is propagated along the waveguides and re-emitted as a magnified image at the output ends of the waveguides (with separation $d > \lambda$). Traditional optics are used to capture the magnified image.

The nanowaveguides can have their input ends located on a planar (as depicted) or curved stage. In this depiction, the distal ends of these diverging waveguides are located on a much

#202388 - $15.00 USD Received 2 Dec 2013; revised 16 Feb 2014; accepted 19 Feb 2014; published 27 Feb 2014
(C) 2014 OSA

larger (also planar or curved) image surface. The light emitted or scattered from the illuminated object ("object") couples to the input ends of the waveguides whose lateral spacing is smaller (even much smaller) than the illumination wavelength λ and propagates as waveguided light or surface plasmon polaritons (SPP), which subsequently re-emit as photons at the output ends of the waveguides, where the spacing is larger than λ. The ratio of the inter-waveguide spacing at the opposite sides of the NFOM determines its magnification. Conventional optics can then be used to capture the magnified output image, making the entire device a nanoscale optical microscope, or nanoscope. While in the original proposal [12] the waveguides were envisioned as nanoscale coaxial transmission lines (nanocoax), here we further explore nanowires and nanogrooves as alternatives. We also investigate a diverging pair of nanowires as a basic building block of our NFOM, illustrating its subwavelength, nanoscopic resolution.

The basic factors considered when selecting an appropriate nanowaveguide for our NFOM were: i) light coupling to the waveguide, ii) attenuation of light or SPPs along the waveguide, iii) inter-waveguide crosstalk, and iv) manufacturability. Depending on the sensitivity of the illuminated object to radiation intensity, there may be an additional constraint placed on the allowed strength of the illumination source, therefore setting a lower limit on the minimum allowable transmission of the device. It has been demonstrated that nanocoaxes can couple to and transmit visible light with relatively long propagation length, estimated to be up to 50 microns [13,14]. These waveguides are expected to have negligible crosstalk, since the propagating light is enclosed entirely within a metallic shield. Similarly, it has been demonstrated that nanowires are capable of transmitting light [15–17]. Ditlbacher, *et al.* [15] showed experimentally that nanowires can be used as waveguides of light energy via SPP modes, with propagation length of at least 20 microns and tight field confinement to the wire. Recently, it has been demonstrated that grooves in metal can also act as nanowaveguides [18,19]. As fabrication of metallic nanowires is less complicated than concentric metal-dielectric-metal nanocoaxes, and surface grooves easier still, we investigated the performance of all these structures. Silver was our material of choice for its relatively low optical loss in the visible.

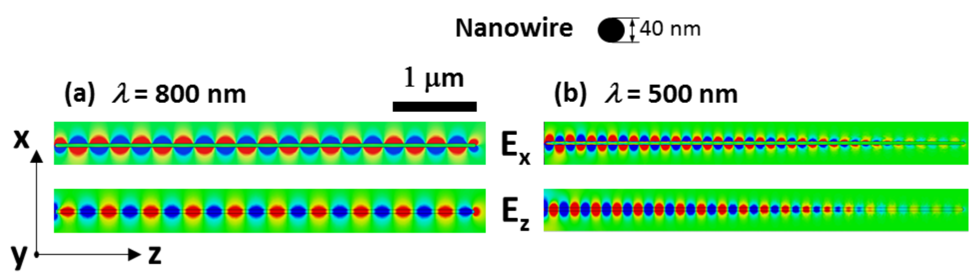

Fig. 2. *X* and *z* components of the electric field along silver nanowires 40 nm in diameter and 5 μm in length, excited with light of vacuum wavelength (a) λ = 800 nm and (b) 500 nm. SPP modes are clearly visible in each case, but with case (b) showing high attenuation over the length of the wire.

To compare nanowaveguide structures, we simulated transmission of light through the aforementioned waveguide architectures by employing the finite element method [20,21]. To excite a waveguide in our NFOM, we use a circular pinhole aperture in a metallic wall (simulated as a sheet of a perfect electrical conductor). A monochromatic wave propagating on one side of the wall produces a dipole-like excitation of the waveguide, placed on the other side of the wall, 10 nm away from the aperture. Figure 2 shows electric field maps for a silver nanowire 40 nm in diameter and 5 μm long taken at wavelengths spanning the visible range, from λ = 500 to 800 nm. Negligible mode attenuation is seen for the λ = 800 nm wavelength, while appreciable reduction occurs for λ = 500 nm. Further simulations have shown that minimal attenuation occurs for λ between 600 and 800 nm. Similar behavior is found for nanowires from 20 nm to 200 nm diameter, generally increasing in transmission with increasing diameter.

From Fig. 2, it is clear that the nanowire mode is SPP with a strongly plasmonic character. This is evidenced by a large, along-the-axis E_z component of the electric field, with large penetration into the nanowire bulk. This causes appreciable metallic loss and, consequently, the large attenuation at λ = 500 nm. The corresponding result for the nanocoax structure is shown in Fig. 3, where relatively less attenuation is seen at 500 nm, due to a smaller plasmonic character of the SPP in this architecture.

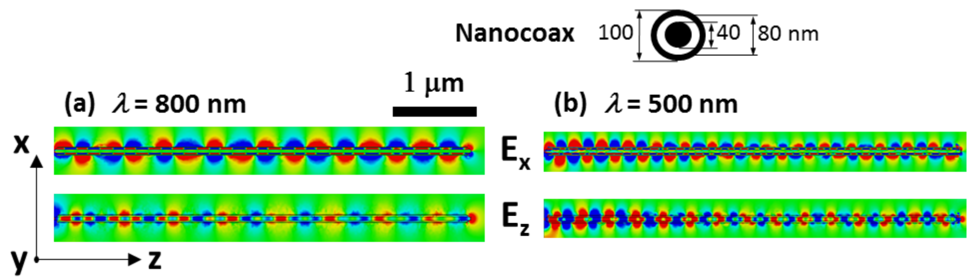

Fig. 3. *X* and *z* components of the electric field along nanocoaxes 5 μm in length, excited with light of vacuum wavelength (a) λ = 800 nm and (b) 500 nm. In both cases, the coaxes have a 40 nm diameter inner silver core, a 20 nm thick vacuum annulus, and a 10 nm thick silver shield. The nanocoax modes appear to be a combination of classical coaxial cable TEM modes and SPP modes. Case (a) shows little attenuation while case (b) shows clear attenuation, albeit less than for the nanowire in Fig. 2(b).

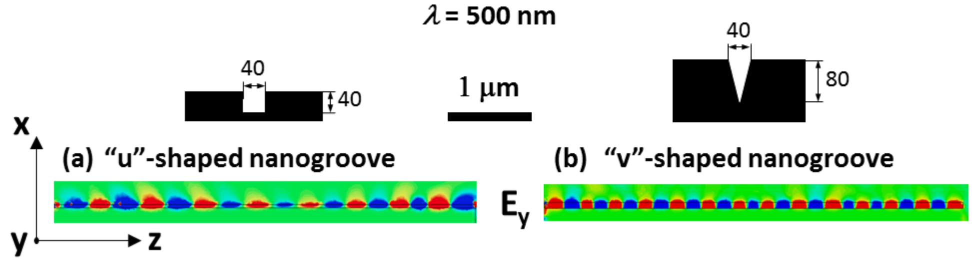

Fig. 4. *Y* components of the electric field along (a) a 40 nm square "u" groove and (b) a 40 nm wide by 80 nm deep "v" groove. Both grooves are 5 μm in length in a silver medium. The excitation in both cases has a vacuum wavelength λ = 500 nm. TEM modes are clearly visible in each case, with no visible attenuation, but with the "u" groove showing some evidence for beating.

The classic analog of this nanoscale waveguide, the conventional coaxial cable, is a non-plasmonic TEM transmission line, and much of that character is retained in the nanocoax, although our coaxes lack perfect enclosure of the light within the coax due to the thinness of the metallic shield. We have also tested two open, "nanogroove" waveguide scenarios, shown in Fig. 4. Here, we find excellent light confinement and negligible attenuation, though only at the 500 nm wavelength shown. The electric field of the transmitted mode is almost entirely the E_y component, *i.e.* it is strongly non-plasmonic, which reduces attenuation due to metallic losses. Above 600 nm, however, attenuation due to radiative loss is large, and the wave is no longer confined to the guide.

In general, we observe excellent wave propagation (in either a plasmonic or photonic regime) along all waveguides studied, at least in certain frequency bands. Furthermore, we studied the effect of perturbations to the nanowire's geometry and found that 10 nm deviations in a wire of 40 nm diameter changed the transmission of the wire by no more than

#202388 - $15.00 USD Received 2 Dec 2013; revised 16 Feb 2014; accepted 19 Feb 2014; published 27 Feb 2014
(C) 2014 OSA

10%. However, there is significant impedance mismatch at the input and the output ends, leading to significant loss of transmission efficiency due to reflections. This mismatch can be strongly reduced (in principle, eliminated) by proper engineering of waveguide terminations (antennae). Techniques might include dielectric grading, diameter modulation, or other antenna schemes, and will be employed in future studies and designs.

In the following study, we chose nanowires as the waveguides of an NFOM. Optical waveguiding in nanowires has recently been demonstrated experimentally [15] and via simulations [17]; in ref [15], 20 µm long nanowires, laser-excited at one end, emitted light from the distal end clearly visible with a conventional optical microscope. Figure 5 shows the geometry of the pair simulated here, as well as field maps for the E_x and E_z components. We chose the nanowires to be 40 nm in diameter and 2 µm in length, with no dielectric coating. The wires were excited with the pinhole described above, with light of vacuum wavelength λ = 800 nm, but with the location of the pinhole aperture varied along the *x*-axis. The input ends of the wires were placed $\lambda/10$ = 80 nm apart (center-to-center), while the distal ends of the wires were separated by 1 µm (center-to-center). Figures 5(a) and 5(c) are for the case of the excitation pinhole directly in front of the upper nanowire, and Figs. 5(b) and 5(d) for the pinhole halfway between the nanowires. Clearly, the excitation location dramatically determines the excitation degree of a given nanowire. This determines the resolution of the system, in this case at least 80 nm, *i.e.* strongly subwavelength.

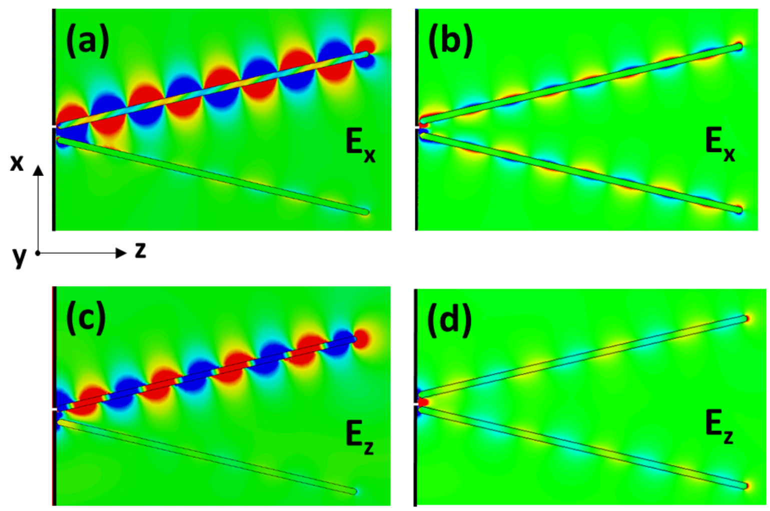

Fig. 5. *X* and *z* components of the electric field in a two nanowire NFOM. The wires are 40 nm in diameter, 2 µm in length, and made of silver. Their close ends are separated by 80 nm, center-to-center, while their distal ends are separated by 1 µm, center-to-center. They are excited by λ = 800 nm vacuum wavelength light, with the aperture positioned adjacent to the center of the top wire ((a) and (c)) or halfway between the two wires ((b) and (d)). Excitation of the top wire results in SPP modes highly localized to that wire alone, while excitation between the wires yields symmetric, low amplitude SPP modes on both wires.

The transmitted power density of a particular wire is at a maximum when the aperture is near that wire and quickly drops to zero away from the wire. We conclude that inter-wire crosstalk in our proposed plasmonic nanowire NFOM is sufficiently low that subwavelength image integrity is maintained at the distal end of the device. The crosstalk issue has been studied previously [17] in a pair of dielectric-coated nanowires placed certain distances apart. The results showed that crosstalk rapidly decayed with increasing inter-wire distance (as trivially expected), and can be further reduced by coating with a dielectric. It is worth noting that the studies we present here were also performed for silver-based nanocoaxes, yielding similar results to the nanowire case.

#202388 - $15.00 USD Received 2 Dec 2013; revised 16 Feb 2014; accepted 19 Feb 2014; published 27 Feb 2014
(C) 2014 OSA

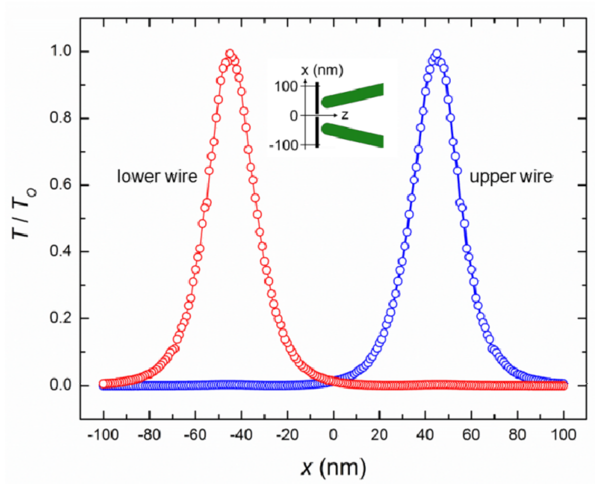

Fig. 6. Calculated normalized transmitted electric field intensity along the converging wires of Fig. 5, as the excitation aperture is moved along the *x*-axis, from halfway between both wires ($x = 0$) to above and below both wires ($x = \pm 100$ nm). This intensity is found by averaging the normalized magnitude of the time-averaged Poynting vector in a cylinder 60 nm in radius surrounding the distal half of the wires. The inset shows the geometry.

The subwavelength resolution of our simulated NFOM is further confirmed in Fig. 6, which plots transmitted field intensity [22] against the location of the pinhole light source. There, it can be seen that each wire only propagates light when the aperture source is localized near its end (*e.g.* centered at x~45 nm for the upper wire, blue data), with negligible light collection/plasmon propagation when the source is move to the adjacent wire (see blue data near x ~–45 nm). The FWHM is about 25 nm for the 40 nm diameter wires employed. This value can be adopted as the spatial resolution for the nanoscope structure. Considering potential issues fabricating precisely controlled-diameter nanowires, we simulated an NFOM with one wire 40 nm and the other 60 nm in diameter and found the device achieved ~90% of the resolution of the symmetric 40 nm device.

In conclusion, we have shown that a near field optical magnifier based on plasmonic nanowires can in principle be used to image subwavelength features. Our simulated device has resolution of ~λ/32 = 25 nm. Such a device could be used in conjunction with conventional optical microscopy for real-time noninvasive imaging of living systems at the nanoscale. We have also shown that the real driver of efficiency for such a device is not propagation decay along the wires — or even precise control of the wires' geometry — but impedance matching into and out of the device.

Acknowledgments

The authors acknowledge support from the W.M. Keck Foundation and assistance from Fan Ye of Boston College.